J. Biochem. 128, 301–307 (2000)

Analyses of Virus-Induced Homomeric and Heteromeric Protein Associations between IRF-3 and Coactivator CBP/p300[1]

Wakako Suhara,[*] Mitsutoshi Yoneyama,[*] Tomokatsu Iwamura,[*] Shoko Yoshimura,[†] Keiko Tamura,[†] Hideo Namiki,[‡] Saburo Aimoto,[†] and Takashi Fujita[*,2]

[*]Department of Tumor Cell Biology, The Tokyo Metropolitan Institute of Medical Science, 3-18-22 Honkomagome, Bunkyo-ku, Tokyo 113-8613; [†]Research Center for Structural Biology, Institute for Protein Research, Osaka University, 3-2 Yamadaoka, Suita, Osaka 565-0871; and [‡]Department of Biology, School of Education, Waseda University, 1-6-1 Nishiwaseda, Shinjuku-ku, Tokyo 169-0051

Received April 28, 2000; accepted May 31, 2000

Cellular genes including the type I interferon genes are activated in response to viral infection. We previously reported that IRF-3 (interferon regulatory factor 3) is specifically phosphorylated on serine residues and directly transmits a virus-induced signal from the cytoplasm to the nucleus, and then participates in the primary phase of gene induction. In this study, we analyzed the molecular mechanism of IRF-3 activation further. The formation of a stable homomeric complex of IRF-3 between the specifically phosphorylated IRF-3 molecules occurred. While virus-induced IRF-7 did not bind to p300, the phosphorylated IRF-3 complex formed a stable multimeric complex with p300 (active holocomplex). Competition using a synthetic phosphopeptide corresponding to the activated IRF-3 demonstrated that p300 directly recognizes the structure in the vicinity of the phosphorylated residues of IRF-3. These results indicated that the phosphorylation of serine residues at positions 385 and 386 is critical for the formation of the holocomplex, presumably through a conformational switch facilitating homodimer formation and the generation of the interaction interface with CBP/p300.

Key words: CBP/p300, IRF-3, phosphorylation, type I interferon, virus infection.

Upon infection by a variety of viruses, type I interferon (IFN-α and IFN-β) genes are activated as an innate response resulting in the secretion of IFNs, which bind to cell surface receptors and induce the expression of a set of genes (Interferon Stimulated Genes; ISGs). Some ISGs have been shown to be responsible for the establishment of an antiviral state. In addition to the defense against viral infections, IFNs exhibit pleiotropic biological activities affecting various physiological functions (*1*, *2*).

Signaling from the type I IFN receptor has been elucidated. The binding of a ligand to the receptor leads to the activation of protein tyrosine kinases Jak1 and Tyk2 in the cytoplasm, which phosphorylate signal transducers and activators of transcription (STAT) 1 and 2, resulting in the generation of trimeric ISG factor 3 (ISGF3). ISGF3 binds to IFN-stimulated response elements (ISRE) and participates in IFN responses (*3*).

It has been postulated that viral infection directly triggers signals that result in gene activation mediated by ISRE or IRF binding motifs, since these genes can be activated in cells defective in IFN signaling. Evidence that IRF-3 and, more recently, IRF-7 participate in gene activation induced by a virus has emerged (*4–16*). Both IRF-3 and IRF-7 need to be phosphorylated in a signal-dependent manner to function. Since IRF-7 accumulation is induced secondarily by autocrine IFN, it may play a major role in the secondary amplification of the gene expression (*5*, *9*, *11*).

In many tissues, IRF-3 accumulates in its inactive form in the cytoplasm due to constitutive export from the nucleus mediated by the functional nuclear export signal (NES) (*15*). The following events were observed after viral infection: IRF-3 was phosphorylated on specific serine residues, translocated to the nucleus, and associated with the coactivator proteins CBP/p300 to form a holocomplex, binding affinity for ISRE or IRF elements (PRDI of IFN-β and VRE-α of IFN-α) being generated. A dominant-negative mutant of IRF-3 inhibits the activation of endogenous type I IFN and ISGs, strongly indicating that IRF-3 is at least one of the primary mediators of virus-induced gene activation (*15*).

Concerning the activation mechanism of IRF-3, Lin *et al.* (*8*) proposed a model based on their observations: (i) in unstimulated IRF-3, the C-terminal domain (residues 380 to 427) interacts with the internal region (residues 98 to 240) and as a result of this intramolecular interaction, DNA binding and dimerization are inhibited. (ii) Virus infection induces multiple phosphorylation of the Ser/Thr cluster (S396, S398, S402, T404, and S405), abrogating the

[1] This work was supported by the Research for the Future Program, the Japan Society for the Promotion of Science, the Ministry of Education, Science, Sports and Culture of Japan, Toray Industries Inc., Nippon Boehringer Ingelheim Co., Ltd., and Kowa Company, Ltd.

[2] To whom correspondence should be addressed. Tel/Fax: +813-3823-6723, E-mail: fujita@rinshoken.or.jp

Abbreviations: IFN, interferon; IRF-3, IFN regulatory factor 3; ISGs, interferon stimulated genes; ISGF3, ISG factor 3; ISRE, IFN-stimulated response elements; PRDI, positive regulatory domain I; NES, nuclear export signal; NDV, Newcastle disease virus; GST, glutathione S transferase; DOC, deoxycholate.

intramolecular inhibition, resulting in a DNA binding-competent dimer of IRF-3 interacting with CBP/p300. This model is based mainly on their observation that the removal (residues 395 to 427) or introduction of amino acid substitutions (5 Ser/Thr to 5 Asp, termed 5D) in the C-terminal domain results in active IRF-3, *i.e.* a DNA binding complex containing the IRF-3 dimer and CBP/p300.

In this study we biochemically analyzed the molecular events following the specific phosphorylation of IRF-3. First, we confirmed that a homomeric association occurs between the specifically phosphorylated molecules of IRF-3. Unlike in previous studies (*7*, *8*), our analyses involving IRF-3 point mutants clearly showed that serine residues 385 and 386, but not the carboxyl terminal serine/threonine cluster, are critical for the interaction as well as their transcriptional activity. We demonstrated that virus-induced IRF-7 did not bind with p300, a condition under which IRF-3 specifically bound with p300, clearly showing the distinct activation mechanisms of IRF-3 and IRF-7. Furthermore, using a synthetic phosphopeptide corresponding to the activated IRF-3 as a binding competitor, we found that p300 recognizes the structure surrounding the phosphorylated serine residues. These results indicated that the phosphorylation of the specific serine residues on IRF-3 triggers the following events leading to gene activation.

MATERIALS AND METHODS

Plasmid Constructs—Expression constructs of pEF-p50-IRF-3 and pEF-HAIRF-3 were described previously (*15*). To generate a deletion mutant of IRF-3 (1-394), HA-tagged IRF-3 cDNA was amplified by PCR and the fragment was inserted into pEF-BOS. Additional point mutations were introduced into cDNA by the Kunkel method. To obtain the mammalian expression vector for GST-human IRF-3 fusion protein, the *Bam*HI–*Not*I fragment of pGEX4T2-IRF-3 (residues 64–427) (*15*) was inserted into pEBgs (GST gene fusion vector derived from pEF-BOS) to generate pEFGSTIRF-3. The GSTIRF-7H (residues 101–516) expression vector (pEFGSTIRF-7H) was constructed by insertion of the *Bss*HII-*Not*I fragment of pCMV.SPORT IRF-7H (*5*) into pEBgs. The HAp300 expression vector (pEFHAp300) was obtained by insertion of the *Not*I-*Cla*I fragment of pLNSX-HA–tagged human p300 into pEF-BOS. The p300 deletion mutant (pEF-HA Δp300;1-192/1752-2221) was obtained by deletion of the *Bsp*HI-*Mun*I fragment from pEF-HA p300 and by insertion of an oligonucleotide containing a stop codon at the *Bst*XI site. To obtain the plasmid DNA for baculovirus expression of GSTΔp300, the *Xba*I fragment of pEF-HAΔp300 (1-192/1752-2221) was inserted into pVLGS (derived from pVL1393) to generate pVLGSΔp300. We thank Drs. D. Livingston and I. Kitabayashi for p300 cDNA, Dr. P.M. Pitha for IRF-7H cDNA, and Dr. B. Mayer for pEBgs and pVLGS. Reporter construct p-55C1BLuc was described elsewhere (*18*).

GST Pull Down Assay—A cell lysate containing GST fusion proteins was incubated with glutathione Sepharose 4B (Pharmacia) at 4 °C for 30 min in lysis buffer. After extensive washing with lysis buffer, the bound proteins were eluted with SDS loading buffer, separated by SDS-PAGE, and then immunoblotted. Immunoblotting was performed as described previously (*15*, *17*).

Recombinant Baculo Virus Encoding GSTΔp300—Sf9 cells were maintained in SF-900IISFM (GIBCO BRL) supplemented with 10% fetal bovine serum. pVLGSΔp300 DNA was transfected into Sf9 cells with BaculoGold baculovirus DNA (PharMingen) by means of CellFECTIN Reagent (GIBCO BRL) to generate recombinant baculovirus. The recombinant virus was used to infect Sf9 cells to produce GSTΔp300.

In Vitro Assay of Binding between IRF-3 and Recombinant GSTΔp300—Baculovirus-infected Sf9 cells were lysed in phosphate-buffered saline (PBS; pH 7.0) supplemented with Triton X-100 (1%), EDTA (0.5 mM), leupeptin (0.1 mg/ml), and phenylmethylsulfonyl fluoride (PMSF; 1 mM). The lysate was centrifuged (15,000 rpm, 10 min), and the supernatant was reacted with glutathione Sepharose 4B (Pharmacia) for 30 min at 4°C, washed and then equilibrated with Lysis buffer (50 mM Tris-HCl, pH 7.5, 150 mM NaCl, 1 mM EDTA and 1% NP-40) supplemented with sodium orthovanadate (1 mM), leupeptin (0.1 mg/ml) and PMSF (1 mM). The cell lysate was then added to the resin, followed by incubating for 5 min. The beads were washed three times with lysis buffer, and then suspended in SDS loading buffer to elute the protein. For competition by peptides, the resin was incubated with peptides (5 μg) for 20 min at 4°C before the addition of the lysate.

Antibodies and Peptides—Anti p50 epitope monoclonal antibody was established by Dr. N. Hanai (Kyowa Hakko Kogyo). This monoclonal antibody reacts strongly with tagged IRF-3, but the reaction with human p50 is below the detectable level. Anti-p300 (Upstate Biotechnology) and anti-GST (Santa Cruz Biotechnology) monoclonal antibodies were obtained commercially. Anti NES antiserum was generated by immunization of a rabbit with the IRF-3 NES peptide (EDILDELLGNMVLA).

Phosphorylated and non-phosphorylated peptides, covering the sequence of IRF-3 (375-427), were prepared by an Fmoc solid-phase method with a peptide synthesizer model 433A (Applied Biosystems, Foster City, CA, USA), adopting software ver. 1.0.1 FastMoc 0.25Ω MonPrevPK. Two phosphoserine residues were introduced using Fmoc-Ser[PO-(OBzl)(OH)]. Peptides were purified by reversed-phase HPLC, and their purities were confirmed by amino acid analyses and MALD-TOF mass analyses. The peptides were finally dissolved in 6 M guanidine and then dialyzed against 20 mM Hepes, pH 7.9.

Luciferase Assay—Luciferase assays were performed as described previously (*18*).

Immunoprecipitation—^{32}P-labeled IRF-3 or mutants were immunoprecipitated as described previously (*15*). The binding reaction was performed in RIPA buffer (50 mM Tris-HCl, pH 7.5, 150 mM NaCl, 1% NP-40, 0.5% DOC, and 0.1% SDS) supplemented with sodium orthovanadate (1 mM), phenylmethylsulfonyl fluoride (PMSF; 1 mM), and leupeptin (20 μg/ml).

RESULTS

Homomeric Complex Formation of IRF-3—It has been reported that the IRF-3 homodimer (*8*) and IRF-3/IRF-7 heterodimer (*13*) are formed after induction. To examine the formation of a homomeric complex of IRF-3, a fusion construct of glutathione S transferase (GST) with IRF-3 (GSTIRF-3) and p50 epitope-tagged IRF-3 (p50IRF-3) or

mutants of it with amino acid substitutions, as described in Fig. 1A, were expressed in mouse L929 cells. Then after mock treatment or induction by infection with Newcastle disease virus (NDV), cell lysates were prepared. The lysates were precipitated with glutathione Sepharose and then the co-precipitated p50IRF-3 was monitored by immunoblot-

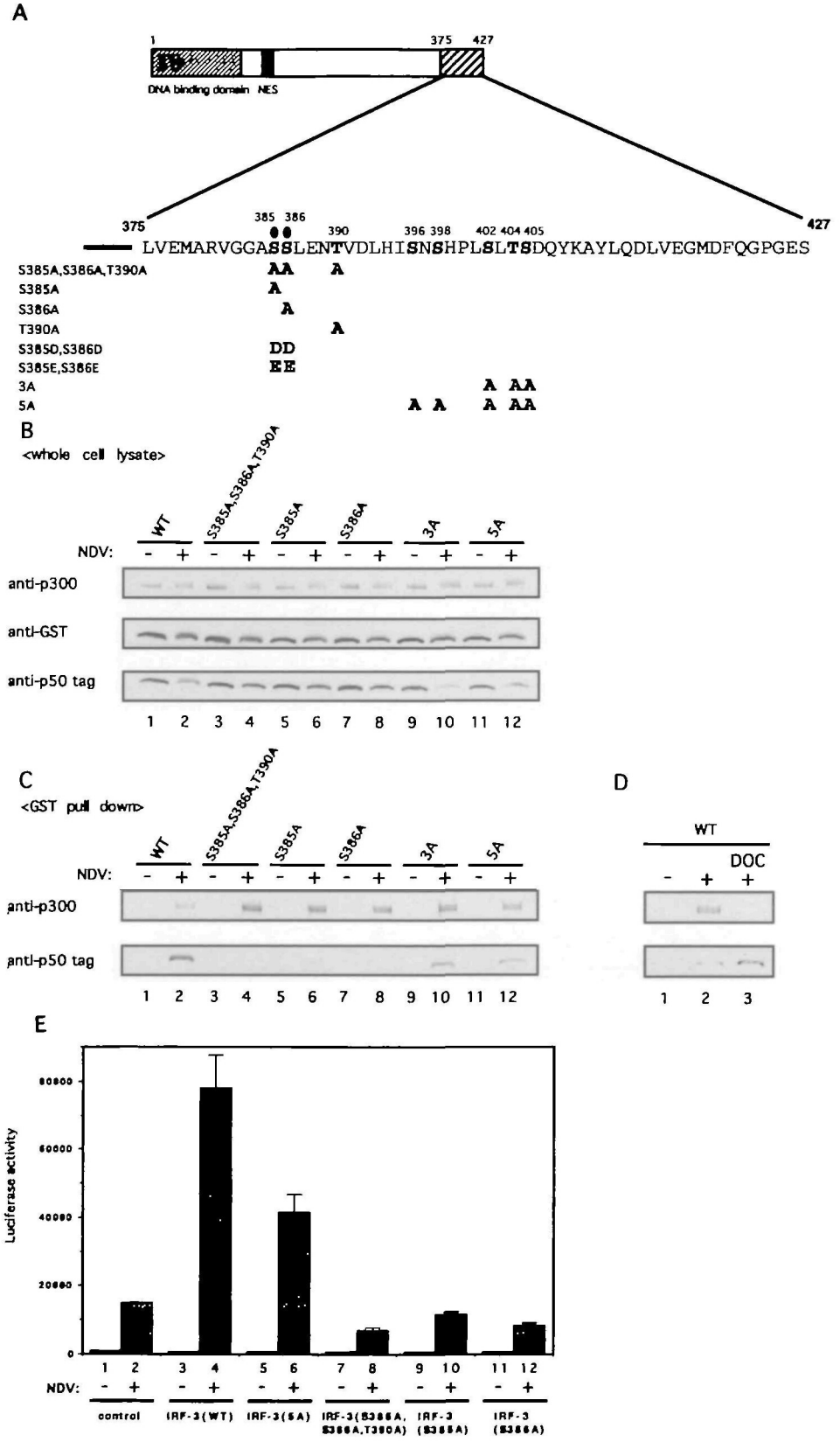

Fig. 1. **Essential role of Ser385 and Ser386 in homomeric complex formation of IRF-3.** (A) Schematic representation of IRF-3 mutants. The primary structure of residues 375–427 is shown. The mutant names (left) and the substituted amino acids (bold letter) are indicated (right). (B) Expression of the GSTIRF-3 and IRF-3 mutants. L929 cells were transiently transfected with the GSTIRF-3 expression vector and either of the p50-tagged IRF-3 or mutants (lanes 1 and 2: wild type; lanes 3 and 4: S385A, S386A, T390A; lanes 5 and 6: S385A; lanes 7 and 8: S386A; lanes 9 and 10: 3A; lanes 11 and 12: 5A). Cells were either mock treated (–) or infected with NDV (+) for 12 h. The whole cell lysates were subjected to immunoblotting using anti-p50 epitope, anti-GST and anti-p300 antibodies, respectively. (C) Detection of the homomeric complex of IRF-3. Whole cell lysates, as indicated in (B), were precipitated with glutathione-Sepharose as described under "MATERIALS AND METHODS." Lanes 1 to 12 correspond to the lanes in (B). Co-precipitated p50-tagged IRF-3 and endogenous p300 were detected by immunoblotting. (D) Dissociation of p300 from the homomeric complex of IRF-3 by DOC treatment. Cells co-expressing GSTIRF-3 and p50-tagged IRF-3 were mock treated (–) or infected with NDV (+). The lysates were precipitated with glutathione-Sepharose in the absence (lanes 1 and 2) or presence of (lane 3) of 1% DOC. The co-precipitated p50-tagged IRF-3 and endogenous p300 were detected by immunoblotting. (E) Effect of IRF-3 mutations of serine/threonine residues on the transcriptional activation potential. L929 cells were transiently transfected with the indicated effector constructs, together with the reporter construct containing repeated PRDI (p-55C1BLuc). The effector constructs were: the control vector (pEF-BOS; lanes 1 and 2), p50-tagged IRF-3 (lanes 3 and 4), and p50-tagged IRF-3 mutants (5A, lanes 5 and 6; S385A, S386A, T390A, lanes 7 and 8; S385A, lanes 9 and 10; S386A, lanes 11 and 12). Luciferase activity was examined at 12h after mock (–) or NDV stimulation (+). Error bars show the standard error for quadruplicate transfections.

ting (Fig. 1). The wild type p50IRF-3 formed a clear complex with GSTIRF-3 after virus induction (Fig. 1C, lanes 1 and 2). This is unlikely to be an artifact due to introduction GST moiety because similar results were obtained when influenza hemagglutinin (HA) tagged IRF-3 was used instead of GSTIRF-3 (data not shown). However, the mutants with substitutions of Ser385 and/or Ser386 did not form a homomeric complex with wild type GSTIRF-3 (lanes 3 to 8). The mutations in 3A and 5A were previously shown to inactivate IRF-3 as to the response to virus infection (*8*), and this was one of the lines of evidence supporting for their model of IRF-3 activation by a virus. However, 3A and 5A clearly formed a complex with wild type IRF-3 after virus induction (lanes 9 to 12), indicating that the phosphorylation of these residues is not essential in contrast with in the case of serines 385 and 386. It is noteworthy that the homomeric complex was stable with 1 M NaCl, 8 M urea, and 1% deoxycholate (DOC) (Fig. 1D and our unpublished observations). Despite the limited primary structure homology, we did not detect a significant association between IRF-3 and IRF-7 under the same conditions (data not shown).

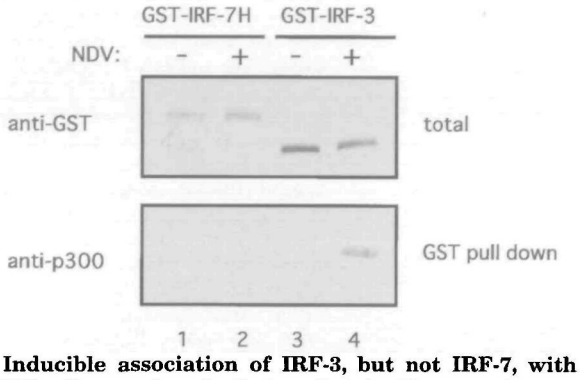

Fig. 2. **Inducible association of IRF-3, but not IRF-7, with p300.** L929 cells were transiently transfected with expression vectors for GSTIRF-7H or GSTIRF-3, and then mock treated (–) or infected with NDV (+) for 12h. The expressed GSTIRF-7H (lanes 1 and 2) and GSTIRF-3 (lanes 3 and 4) were detected by immunoblotting using anti-GST antibodies (Total: upper panel). GST fusion proteins were precipitated with glutathione-Sepharose as described under "MATERIALS AND METHODS." Co-precipitated endogenous p300 was detected by immunoblotting with anti-p300 antibodies (lower panel).

The complex formed with the GSTIRF-3 was analyzed using an anti-p300 antibody (Fig. 1C, upper lanes). p300 specifically associated with GSTIRF-3 after virus induction. The binding between p300 and phosphorylated IRF-3 is stable with high salt (1 M NaCl) or 8 M urea treatment (data not shown). We found that the addition of DOC (1%) selectively abrogated the association of p300 with IRF-3, leaving the homomeric interaction unchanged (Fig. 1D). Interestingly, the effect of DOC was reversible, and p300 and phosphorylated IRF-3 reassociated after removal of the DOC (data not shown).

As shown above, mutant 5A formed a homomeric complex after virus infection in L929 cells. To explore its transactivation potential, we transfected the IRF-3 expression vector with a reporter luciferase construct containing multimerized PRDI (p-55C1BLuc) in to L929 cells (Fig. 1E). As shown previously (*15*), the expression of the reporter was enhanced by NDV due to the function of endogenous IRFs, and ectopic expression of wild type IRF-3 augmented the expression level about 5-fold without affecting the basal level (lanes 1 to 4). The IRF-3 (5A) significantly augmented the induced expression of the reporter (lanes 5 and 6), albeit less efficiently than the wild type, in correlation with the less efficient formation of the holocomplex (Fig. 1C, lanes 2 and 12). The mutants with substitutions at Ser385 and/or Ser386 did not exhibit transactivation potential (lanes 7 to 12).

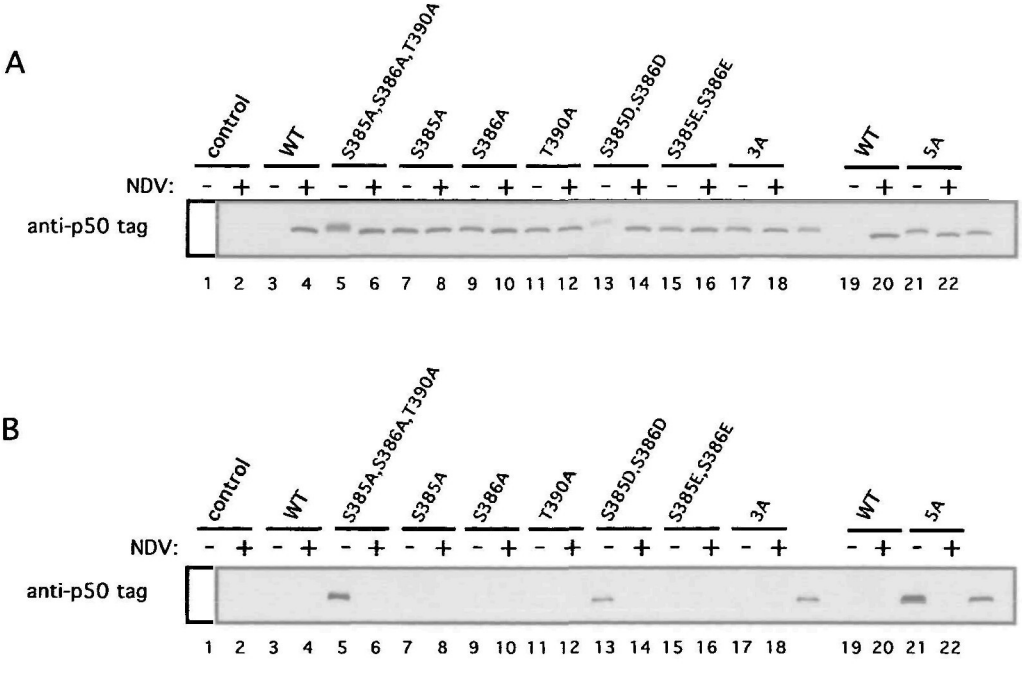

Fig. 3. **Effect of C-terminal serine/threonine substitutions of IRF-3 on inducible association with p300.** (A) Expression of human IRF-3 and mutants in L929 cells. L929 cell were transiently transfected with the empty vector or expression vectors for p50-tagged IRF-3 and the mutants, and then mock treated (–) or infected with NDV (+) for 12h. Lanes 1 and 2: vector, pEF-BOS; lanes 3, 4, 19 and 20: wild type IRF-3; lanes 5 and 6: S385A, S386A, T390A; lanes 7 and 8: S385A; lanes 9 and 10: S386A; lanes 11 and 12: T390A; lanes 13 and 14: S385D, S386D; lanes 15 and 16: S385E, S386E; lanes 17 and 18: 3A; lanes 21 and 22: 5A. Crude lysates of these cells were subjected to immunoblotting with anti-p50 epitope antibodies. (B) Complex formation of IRF-3 mutants with p300. Whole cell lysates from (A) were subjected to the binding assay with GSTΔp300 ("MATERIALS AND METHODS"). The bound IRF-3 was detected by immunoblotting with anti-p50 epitope antibodies. Lanes, as in (A).

These results reemphasize that the phosphorylation of Ser385 and Ser386 is essential for both homodimerization and transactivation, and that the C-terminal serine/threonine residues have an accessory function.

IRF-7 Does Not Form a Stable Complex with p300—IRF-3 and IRF-7 have been shown to be converted to transcriptionally active forms through phosphorylation induced by viral infection (*7, 9–11, 13, 15*). To determine whether or not these IRFs are activated through a common molecular mechanism after phosphorylation by virus stimulation, we investigated the interaction between IRF-7 and p300. IRF-3 and IRF-7 were, respectively, expressed in L929 cells as fusion constructs with GST, and the cells were infected or not infected with a virus (Fig. 2). The GST fusion constructs were precipitated with glutathione Sepharose and then the co-precipitated p300 was detected by immunoblotting. IRF-7 did not form a significant complex with p300 under these conditions. The results show the clearly distinct activation mechanisms of IRF-3 and IRF-7.

Binding of the Phosphorylated IRF-3 with p300—To analyze the interaction between phosphorylated IRF-3 and p300, we developed an *in vitro* assay. First, we delineated that a fragment of p300 with 470 amino acids (residues 1752–2221), which coincides with the glutamine-rich region, contains an interaction site for IRF-3 in co-precipitation experiments (M.Y., unpublished data). A similar region of CBP (1992–2441) was reported to interact with IRF-3 (*7*). GSTΔp300 fusion protein, which contains the above residues, was produced by insect cells ("MATERIALS AND METHODS") and immobilized on glutathione Sepharose beads. The resin was mixed with an extract of L929 cells which had been transfected with the human IRF-3 (hIRF-3) expression vector and then mock-treated or infected with a virus. The bound IRF-3 was separated from the unbound IRF-3 by washing and detected by immunoblotting. Since hIRF-3 was overexpressed due to transient transfection, the molar amount of hIRF-3 exceeded that of endogenous CBP/p300 in this experiment. However, as previously

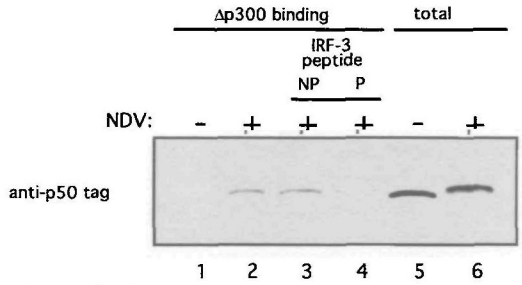

Fig. 4. **A synthetic phosphopeptide can compete with the binding between phosphorylated IRF-3 and p300.** p50-tagged human IRF-3 was expressed in mock-treated (–; lanes 1 and 5) or NDV-infected (+; lanes 2, 3, 4 and 6) L929 cells, as in Fig. 3. The whole cell lysates were subjected directly to immunoblotting (lanes 5 and 6) or the binding assay with GSTΔp300 in the absence (lanes 1 and 2) or presence of synthetic peptides (lane 3: unphosphorylated peptide; lane 4: the peptide phosphorylated at Ser385 and Ser386; "MATERIALS AND METHODS"). The bound IRF-3 was detected by immunoblotting.

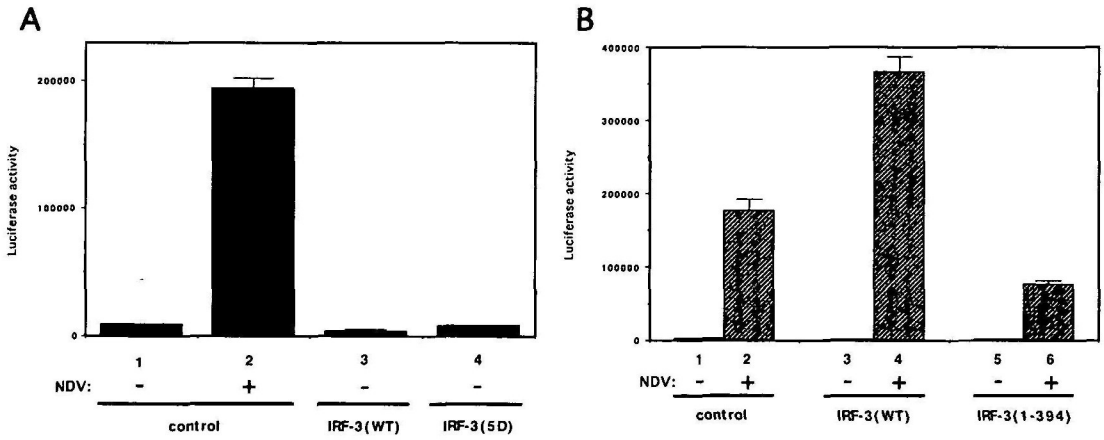

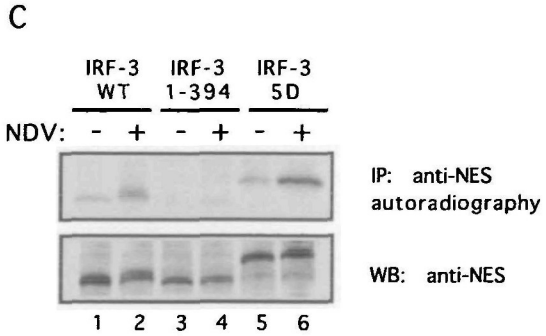

Fig. 5. **IRF-3 mutants (5D and 1–394) are not constitutively active in L929 cells.** (A) Transactivation potential of IRF-3 5D. L929 cells were transiently transfected with a reporter construct containing multimerized PRDI (p-55C1BLuc) with either the control vector (pEF-BOS, lanes 1 and 2) or the expression plasmid for the p50-tagged IRF-3 (WT, lane 3) or p50-tagged point mutant (5D, lane 4). Cells were mock treated (–) or treated with NDV for 12h (+), and then subjected to the luciferase assay. Error bars show the standard error for quadruplicate transfections. (B) Transactivation potential of IRF-3 (1-394). L929 cells were transiently transfected with a reporter construct (p-55C1BLuc) with either the control vector (pEF-BOS, lanes 1 and 2) or the expression plasmid for the HA-tagged IRF-3 (WT, lanes 3 and 4) or HA-tagged deletion mutant (1-394, lanes 5 and 6). Cells were mock treated (–) or treated with NDV for 12h (+), and then subjected to the luciferase assay. Error bars show the standard error for quadruplicate transfections. (C) *In vivo* phosphorylation of IRF-3 5D and IRF-3 (1-394). L929 cells transfected with pEF-p50IRF-3 (WT, lanes 1 and 2), pEF-HAIRF-3 (1-394, lanes 3 and 4), or pEF-p50IRF-3 (5D, lanes 5 and 6) were mock treated (–) or infected with NDV (+), and then cultured for 12 h in the presence of [^{32}P]phosphate. IRF-3 was immunoprecipitated with anti-NES antibodies and separated by SDS-PAGE, and then the phosphorylation of IRF-3 was examined by autoradiography (upper panel). The whole cell lysate was subjected to immunoblotting using anti-NES antibodies (lower panel).

reported, virtually all hIRF-3 molecules showed a change in gel mobility after viral infection, indicating that they are specifically phosphorylated (*15*). The hIRF-3 from infected cells selectively bound to the recombinant p300 indicating that the phosphorylation of IRF-3 is necessary for the interaction (Fig. 3B, lanes 3 and 4). Mutants which have substitutions at potential phosphorylation sites (Fig. 1A) were examined. As we reported earlier, mutation of the serines at positions 385 and/or 386 to alanine abolished the mobility change (Fig. 3A, lanes 5 to 10). At the same time, interaction with p300 was also undetectable (Fig. 3B, lanes 5 to 10). Changes of these serines to acidic amino acids (S385D/S386D or S385E/S386E) also abolished the inducible binding with p300 (Fig. 3B, lanes 13 to 16), indicating that the presence of a negative charge at these positions is not sufficient for the interaction. These results show that phosphorylation of serine residues 385 and 386 is critical for specific binding with p300. On the other hand, mutations of the neighboring serine and threonine residues (T390A, 3A and 5A) did not abolish either the gel mobility change or the binding with p300 (Fig. 3A and B, lanes 11 and 12, and 17 to 22). It is worth noting, however, that 5A binds to p300 less efficiently than the wild type, suggesting that these serines are phosphorylated and participate in the increase in the binding affinity.

Phosphorylated Residues of IRF-3 Directly Participate in the Interaction with p300—To further elucidate the role of serine residues 385 and 386, we chemically synthesized a peptide corresponding to amino acids 375 to 427 with phosphate groups on serines 385 and 386. As a control, an unphosphorylated peptide was also prepared. The peptide's ability to compete with the binding of IRF-3 to p300 was assayed *in vitro*. Figure 4 shows that the phosphorylated peptide but not the unphosphorylated peptide prevented IRF-3 from binding to p300. The peptide did not affect the homomeric IRF-3 complex under the same conditions (unpublished observation). The result indicates that the phosphorylated 53 mer peptide is sufficient for the specific recognition, and that the phosphorylation of residues 385 and 386 is conditional for the recognition.

IRF-3 5D and IRF-3 (1-394) are Not Constitutively Active in L929 Cells—Lin *et al.* (*8*) showed that removal of the C-terminal residues of IRF-3 [IRF-3 (1-394)] or substitution of the C-terminal serine/threonine cluster with aspartic acids [IRF-3(5D)] resulted in constitutive active IRF-3 when expressed in 293 cells. The function of these mutants was examined in our cell system using a multimerized PRDI luciferase reporter which exhibited low basal and high (>20 fold) virus-induced expression (Fig. 5A, lanes 1 and 2). As repeatedly shown, wild type IRF-3 did not affect the basal level of reporter expression (Fig. 5A, lanes 1 and 3). The expression of IRF-3 (5D) did not augment the basal expression level either. Since comparable levels of the wild type IRF-3 and IRF-3 (5D) proteins were expressed (Fig. 5C), we conclude that IRF-3 (5D) was not constitutively active in L929 cells. It is noteworthy that IRF-3 (5D) was hyper-phosphorylated in virus-infected cells as the wild type was (Fig. 5C, lanes 5 and 6).

Likewise, IRF-3 (1-394), which was expressed at a comparable level to the wild type (Fig. 5C, lanes 3 and 4), did not enhance the basal expression of the reporter (Fig. 5B). In contrast to the wild type IRF-3, IRF-3 (1-394) did not transactivate after virus induction and even reduced the induced expression (Fig. 5B). Consistent with this, IRF-3 (1-394) was only very weakly phosphorylated as compared with the wild type IRF-3 (Fig. 5C, lanes 3 and 4). We do not have a conclusive explanation for the inefficient phosphorylation. Presumably the C-terminal segment is necessary for the recognition by kinase(s).

DISCUSSION

In this study, we investigated the molecular mechanism of IRF-3 activation induced by viral infection.

The first step, which is not yet well characterized, is the phosphorylation of serine residues present in the carboxyl terminal region of IRF-3, particularly Ser385 and Ser386. Evidence argues against the involvement of PKR, JNK and IKK, which are activated as a consequence of viral infection or dsRNA treatment (*14*, *19*).

The phosphorylation of IRF-3 may induce a conformational change that facilitates the formation of a homomeric complex because no additional component has so far been detected and the phosphopeptide of IRF-3 did not affect the homomeric complex (data not shown). Among the IRF family proteins, homomeric complex formation is unique to IRF-3, for example, IRF-1 and IRF-2 bind to DNA as monomers or a heterodimer with ICSBP (*20–22*). Furthermore, unlike many transcription factors which recognize the target palindromic DNA sequences as a dimer, much of the recognition sequence of IRF-3 consists of direct repeats. Interestingly, the ISRE of ISG15, which is commonly used for the binding assay for IRF-3, contains core motifs sufficient for binding with two molecules of IRF, as judged from the crystal structure of IRF-2 bound to the IFN-β enhancer. In the case of IRF-2, binding cooperativity to the tandem sites is observed, consistent with the determined crystal structure of the protein/DNA complex (*22*). Therefore, homomeric complex formation may be advantageous for precise and stable recognition of tandem repeat IRF motifs, as found in the IFN-β enhancer. We examined palindromic as to for binding with the holocomplex of IRF-3, however, unlike with the ISG15 site, no significant binding was observed (unpublished observation). Although the precise stoichiometry of IRF-3 within the complex was not determined, our preliminary results on native gel electrophoresis in the presence of DOC suggest that most of it is present as a dimer. Therefore the structure of IRF-3 complexed with its binding site should not be in dyad symmetry. A possible precedent for dimeric recognition of the tandem repeat motifs is the GCNF homodimer (*23*).

Lin *et al.* (*8*) propose an intramolecular interaction between residues (98 to 240) and (380 to 427) of IRF-3, and this interaction results in inhibition of homodimer formation and DNA binding. According to their model, the inhibition is reversed on the removal of residues (395 to 427) or phosphorylation of Ser/Thr clusters present within. However, our results showed that serines 385 and 386 are critical for the homomeric complex as well as the holocomplex. Furthermore, neither 5D nor IRF-3 (1-394) was constitutively active in L929 cells (Fig. 5). The discrepancies may be due to the different cell/virus combination and assays. However, we have no conclusive evidence explaining these discrepancies so far. Apparently more work, particularly elucidation of the three-dimensional structure of the IRF-3 molecule, is required to unequivocally understand the

molecular suppression mechanism.

As shown previously, CBP/p300 is an essential component for the DNA binding competent IRF-3 holocomplex (*15*). The induction of the DNA binding activity of an activator molecule through the association of the co-activator CBP/p300 is quite unique to IRF-3. This likely facilitates the dramatic switching on/off of the type I interferon genes. Although we analyzed p300 in the present study, CBP may behave similarly in IRF-3 activation (*15*). The phosphopeptide competition experiment showed that p300 directly recognizes an IRF-3 moiety including the phosphorylated serine residues. Thus the phospholylation of serines 385 and 386 may induce the homomeric and heteromeric interactions through conformational change and generation of an interaction interface, respectively. Phosphorylation dependent recognition between phosphorylated CREB and CBP has been established (*24*). The phosphorylated CREB domain (pKID) interacts with the KIX domain of CBP (*25, 26*). However, the glutamine rich region with which IRF-3 interacts is distinct from the KIX domain, and no primary structure similarity can be found between pKID and IRF-3 (residues 375 to 427), suggesting a new class of phosphorylation dependent transcription factor-coactivator interaction.

REFERENCES

1. DeMaeyer, E. and DeMaeyer-Guignard, J. (1988) *Interferons and Other Regulatory Cytokines*, John Wiley and Sons, New York
2. Sen, G.C. and Lengyel, P. (1992) The interferon system: A bird's eye view of its biochemistry. *J. Biol. Chem.* **267**, 5017–5020
3. Darnell, J.E., Jr., Kerr, I.M., and Stark, G.R. (1994) Jak-STAT pathways and transcriptional activation in response to IFNs and other extracellular signaling proteins. *Science* **264**, 1415–1421
4. Au, W.-C., Moore, P.A., Lowther, W., Juang, Y.-T., and Pitha, P.M. (1995) Identification of a member of the interferon regulatory factor family that binds to the interferon-stimulated response element and expression of interferon-induced genes. *Proc. Natl. Acad. Sci. USA* **92**, 11657–11661
5. Au, W.-C., Moore, P.A., LaFleur, D.W., Tombal, B. and Pitha, P.M. (1998) Characterization of the interferon regulatory factor-7 and its role in the transcription activation of interferon A genes. *J. Biol. Chem.* **273**, 29210–29217
6. Juang, Y.-T., Lowther, W., Kellum, M., Au, W.C., Lin, R., Hiscott, J., and Pitha, P.M. (1998) Primary activation of interferon A and interferon B gene transcription by interferon regulatory factor 3. *Proc. Natl. Acad. Sci. USA* **95**, 9837–9842
7. Lin, R., Heylbroeck, C., Pitha, P.M., and Hiscott, J. (1998) Virus-dependent phosphorylation of the IRF-3 transcription regulates nuclear translocation, transactivation potential, proteasome-mediated degradation. *Mol. Cell. Biol.* **18**, 2986–2996
8. Lin, R., Mamane, Y., and Hiscott, J. (1999) Structural and functional analysis of interferon regulatory factor 3: localization of the transactivation and autoinhibitory domains. *Mol. Cell. Biol.* **19**, 2465–2474
9. Marie, I., Durbin, J.E., and Levy, D.E. (1998) Differential viral induction of distinct interferon-α genes by positive feedback through interferon regulatory factor-7. *EMBO J.* **17**, 6660–6669
10. Sato, M., Tanaka, N., Hata, N., Oda, E., and Taniguchi, T. (1998) Involvement of the IRF family transcription factor IRF-3 in activation of the IFN-β gene. *FEBS Lett.* **425**, 112–116
11. Sato, M., Hata, N., Asagiri, M., Nakaya, T., Taniguchi, T., and Tanaka, N. (1998) Positive feedback regulation of type I IFN genes by the IFN-inducible transcription factor IRF-7. *FEBS Lett.* **441**, 106–110
12. Schafer, S.L., Lin, R., Moore, P.A., Hiscott, J., and Pitha, P.M. (1998) Regulation of type I interferon gene expression by interferon regulatory factor-3. *J. Biol. Chem.* **273**, 2714–2720
13. Wathelet, M.G., Lin, C.H., Parekh, B.S., Ronco, L.V., Howley, P.M., and Maniatis, T. (1998) Virus infection induces the assembly of coordinately activated transcription factors on the IFN-β enhancer *in vivo*. *Mol. Cell.* **1**, 507–518
14. Weaver, B.K., Kumar, K.P., and Reich, N.C. (1998) Interferon regulatory factor 3 and CREB-binding protein/p300 are subunits of double-stranded RNA-activated transcription factor DRAF1. *Mol. Cell. Biol.* **18**, 1359–1368
15. Yoneyama, M., Suhara, W., Fukuhara, Y., Fukuda, M., Nishida, E., and Fujita, T. (1998) Direct triggering of the type I interferon system by virus infection: activation of a transcription factor complex containing IRF-3 and CBP/p300. *EMBO J.* **17**, 1087–1095
16. Yeow, W.-S., Au, W.-C., Juang, Y.-T., Fields, C.D., Dent, C.L., Gewert, D.R., and Pitha, P.M. (2000) Reconstitution of virus-mediated expression of interferon α genes in human fibroblast cells by ectopic interferon regulatory factor-7. *J. Biol. Chem.* **275**, 6313–6320
17. Watanabe, N., Iwamura, T., Shinoda, T., and Fujita, T. (1997) Regulation of NFKB1 proteins by the candidate oncoprotein BCL-3: generation of NF-κB homodimers from the cytoplasmic pool of p50-p105 and nuclear translocation. *EMBO J.* **16**, 3609–3620
18. Yoneyama, M., Suhara, W., Fukuhara, Y., Sato, M., Ozato, K., and Fujita, T. (1996) Autocrine amplification of type I interferon gene expression mediated by interferon stimulated gene factor 3 (ISGF3). *J. Biochem.* **120**, 160–169
19. Chu, W.-M., Ostertag, D., Li, Z.-W., Chang, L., Chen, Y., Hu, Y., Williams., Perrault, J., and Karin, M. (1999) JNK2 and IKKβ are required for activating the innate response to viral infection. *Immunity* **11**, 721–731
20. Bovolenta, C., Driggers, P.H., Marks, M.S., Medin, J.A., Politis, A.D., Vogel, S.N., Levy, D.E., Sakaguchi, K., Appella, E., Coligan, J.E., and Ozato, K. (1994) Molecular interactions between interferon consensus sequence binding protein and members of the interferon regulatory factor family. *Proc. Natl. Acad. Sci. USA* **91**, 5046–5050
21. Escalante, C.R., Yie, J., Thanos, D., and Aggarwal, A.K. (1998) Structure of IRF-1 with bound DNA reveals determinants of regulation. *Nature* **391**, 103–106
22. Fujii, Y., Shimizu, T., Kusumoto, M., Kyogoku, Y., Taniguchi, T., and Hakoshima, T. (1999) Crystal structure of an IRF-DNA complex reveals novel DNA recognition cooperative binding to a tandem repeat of core sequences. *EMBO J.* **18**, 5028–5041
23. Greschik, H., Wurtz, J.M., Hublitz, P., Köhler, F., Moras, D., and Schüle, R. (1999) Characterization of the DNA-binding and dimerization properties of the nuclear orphan receptor germ cell nuclear factor. *Mol. Cell. Biol.* **19**, 690–703
24. Chrivia, J.C., Kwok, R.P., Lamb, N., Hagiwara, M., Montminy, M.R., and Goodman, R.H. (1993) Phosphorylated CREB binds specifically to the nuclear protein CBP. *Nature* **365**, 855–859
25. Parker, D., Ferreri, K., Nakajima, T., LaMorte, V.J., Evans, R., Koerber, S.C., Hoeger, C., and Montminy, M.R. (1996) Phosphorylation of CREB at Ser-133 induces complex formation with CREB-binding protein *via* a direct mechanism. *Mol. Cell. Biol.* **16**, 694–703
26. Radhakrishnan, I., Perez-Alvarado, G.C., Parker, D., Dyson, H.J., Montminy, M.R., and Wright, P.E. (1997) Solution structure of the KIX domain of CBP bound to the domain of CREB: a model for activator:coactivator interactions. *Cell.* **91**, 741–752